Ultrafast broadband optical modulation in indium tin oxide/titanium dioxide 1D photonic crystal

J. Eur. Opt. Society-Rapid Publ. 2022, **18**, 8

https://doi.org/10.1051/jeos/2022009
Available online at: jeos.edpsciences.org

Journal of the European Optical Society-Rapid Publications

RESEARCH ARTICLE OPEN ACCESS

Ultrafast broadband optical modulation in indium tin oxide/titanium dioxide 1D photonic crystal

Liliana Moscardi[1,2], Stefano Varas[3], Alessandro Chiasera[3], Francesco Scotognella[1,2,*], and Michele Guizzardi[1]

[1] Dipartimento di Fisica, Politecnico di Milano, Piazza Leonardo da Vinci 32, 20133 Milano, Italy
[2] Center for Nano Science and Technology@PoliMi, Istituto Italiano di Tecnologia (IIT), Via Giovanni Pascoli, 70/3, 20133 Milan, Italy
[3] Istituto di Fotonica e Nanotecnologie IFN – CNR, Via alla Cascata, 56/C, 3812 Povo – Trento, Italy

Received 24 May 2022 / Accepted 27 August 2022

Abstract. Photonic crystals can integrate plasmonic materials such as Indium Tin Oxide (ITO) in their structure. Exploiting ITO plasmonic properties, it is possible to tune the photonic band gap of the photonic crystal upon the application of an external stimuli. In this work, we have fabricated a one-dimensional multilayer photonic crystal alternating ITO and Titanium Dioxide (TiO_2) via radio frequency sputtering and we have triggered its optical response with ultrafast pump-probe spectroscopy. Upon photoexcitation, we observe a change in the refractive index of ITO. Such an effect has been used to create a photonic crystal that changes its photonic bandgap in an ultrafast time scale. All optical modulation in the visible region, that can be tuned by designing the photonic crystal, has been demonstrated.

Keywords: Indium tin oxide, Ultrafast spectroscopy, Photonic crystal.

1 Introduction

Photonic Crystals (PCs) represent a class of periodic structures that can be integrated into a wide range of technologies. Thanks to their high symmetry (in one, two or three dimensions) and the difference in terms of refractive indices of the constituent materials, an interference of the incident and diffused electromagnetic wave is generated, causing the formation of a forbidden band for the passage of photons, called Photonic Band Gap (PBG) [1–4]. This attributes to PCs their peculiar optical properties and the generation of their changing colors, called structural colors. There are several applications in which multilayer PCs can be exploited, such as distributed feedback lasers [5–8], perfect absorbers [9, 10], and sensors [11–15]. PCs can be fabricated with several techniques in one dimension, two dimensions and three dimensions [16]. Moreover, quasicrystals [17] and disordered structures [18, 19] can be fabricated. Selecting responsive materials for their fabrication, it is possible to modulate their optical response upon application of external stimuli.

Multilayer PCs, also called Distributed Bragg Reflectors (DBRs), that include Indium Tin Oxide (ITO) are promising devices since this plasmonic material is able to show a high refractive index change with an applied electric field [20]. ITO-based DBRs take advantage of the ability to change their refractive index through the application of an electric field in order to modulate the position of the PBG. The optical properties of the multilayer can be easily tuned by acting on the refractive index of the constituent materials or on the geometric parameters of the lattice [21, 22].

In this work we have fabricated a one dimensional PC made by ITO and TiO_2 via radiofrequency sputtering. The fabricated multilayer PC shows a very high optical quality with a strong PBG. By pumping the PC at 1550 nm, in the range of the plasma frequency of ITO, we observe in transient differential transmission measurements relaxation dynamics within the first picosecond of time delay. Such dynamics is mainly due to electron-phonon scattering in ITO. The ultrafast modulation of the plasma frequency of ITO results in an ultrafast modulation of the PBG of the ITO-based PC.

2 Experimental methods

2.1 Sample preparation

The multilayer ITO/TiO_2 structures were deposited on vitreous silica glass (v-SiO_2) by RF magnetron sputtering. The v-SiO_2 substrates have dimensions 75 mm × 25 mm × 1 mm. Before deposition, the substrates were ultrasonically cleaned in deionized water then they were

* Corresponding author: francesco.scotognella@polimi.it

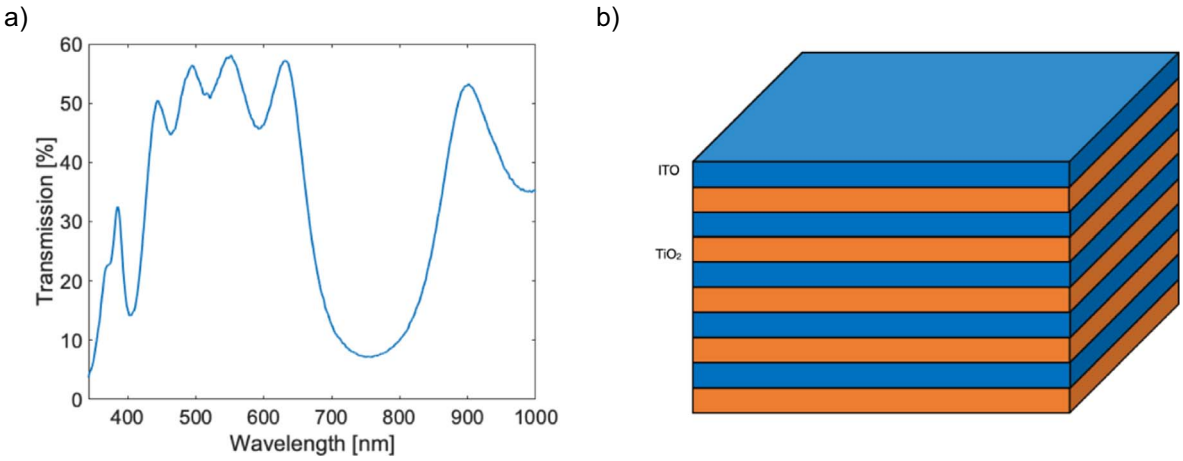

Figure 1. a) Steady-state transmission spectrum of the ITO/TiO_2 PC. b) Sketch of the one-dimensional multilayer PC.

cleaned with ethanol and finally dried in nitrogen. The substrates were after cleaned inside of the RF sputtering chamber for 10 min just before starting the deposition while heating up the temperature to 120 °C at a pressure of 10^{-6} mbar. The magnetron Radio Frequency (RF) sputtering deposition of ITO and TIO_2 films was performed by alternatively changing a 15 cm × 5 cm ITO and 15 cm × 5 cm TiO_2 targets. The residual pressure before the deposition was 4.5×10^{-7} mbar. During the deposition procedure, the substrates were not heated, and the sample holder temperature was kept at 30 °C. The sputtering was performed in an Argon (Ar) atmosphere (5.4×10^{-3} mbar) and an RF power of 110 W was applied on TiO_2 target and 80 W applied on the ITO target. To monitor the thickness of the layers during the deposition, two quartz microbalances INFICON model SQM-160, faced on the two targets were employed. The final resolution on the effective thickness obtained by these quartz microbalances is about 1 Å. More details are available in reference [19]. The deposited structure consists of 5 couple ITO/TiO_2 for a total of 10 layers. The first layer deposited directly on the substrates is ITO while the last layer is TiO_2. Reference ITO and TIO_2 single layer were also fabricated using the same deposition protocol on silicon and vitreous silica glass substrates.

2.2 Optical characterization

The steady-state light transmission spectrum of the PC has been acquired with a JASCO spectrophotometer. The ultrafast differential transmission measurements (Fig. S4) have been performed by using a Coherent Libra amplified laser system with the fundamental wavelength at 800 nm, a pulse duration of about 100 fs and a repetition rate of 1 kHz. Noncollinear optical parametric amplifiers to tune the pump wavelength has been built with a procedure reported in Reference [23] with a fluence of 300 uJ/cm^2. White light generation for the probe pulse has been achieved focusing the fundamental beam into a sapphire plate. The differential transmission $\Delta T/T = T_{ON} - T_{OFF}/T_{OFF}$ has been acquired with an optical multichannel analyzer. T_{ON} and T_{OFF} indicate the probe spectra transmitted the excited and unperturbed sample, respectively. Pump and probe were impinging on the sample at near normal incidence. It is worth mentioning that one-dimensional PCs are polarization insensitive at normal incidence.

3 Results and discussion

In Figure 1a the transmission of the photonic crystal made of 5 bilayers of ITO/TiO_2 is shown, with a decrease of transmittivity below 400 nm due to intragap state of ITO [24] and the more evident decrease where we have the band gap transition around 340 nm. Such decrease in transmission is also related to the edge of the band gap of TiO_2, which is between 330 nm [25] and 400 nm [26]. Moreover, also glass absorption, mainly to due to silicon dioxide interband absorption, contributes to the transmission decrease below 400 nm. As we discussed above the stacking of two dielectric materials (ITO and TiO_2) creates a PBG in the spectral region between 700 and 800 nm. To estimate the thickness of the layers we have performed a fit of the experimental data with the transfer matrix method [27]. In the Supporting Information we report the fit of the transmission spectrum (Fig. S4). For TiO_2 we have used the refractive index dispersion reported in Reference [28]. For ITO, we have used a Drude model with parameters taken from Ref. [29] (i.e., $\varepsilon_\infty = 4$, $N = 2.49 \times 10^{26}$ charge/m^3, $\Gamma = 0.1132$ eV, that are, respectively, the high frequency dielectric constant, the number of carriers, the carrier damping). The contribution of ITO to the transmission spectrum is reported in Figures S2 and S3. The extracted thickness of the ITO layers is 100 nm and the extracted thickness of the TiO_2 layers is 79 nm. Thus, the total thickness of the PC is 895 nm.

It is noteworthy to study how the transmission through the PC change upon photoexcitation of the plasmon. To do so, we have tuned an optical parametric amplifier, used as excitation, at 1550 nm where the ITO shows a strong absorption [29]. After the excitation of the plasmon in a timescale of about 10 fs due to electron scattering we can

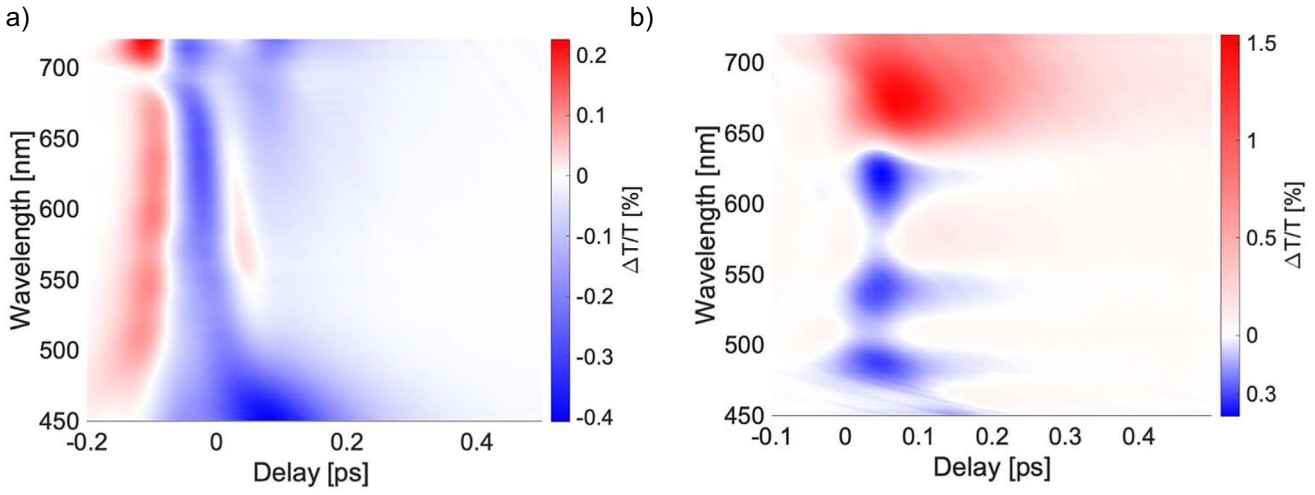

Figure 2. a) Transient response of ITO. b) Transient response of the PC.

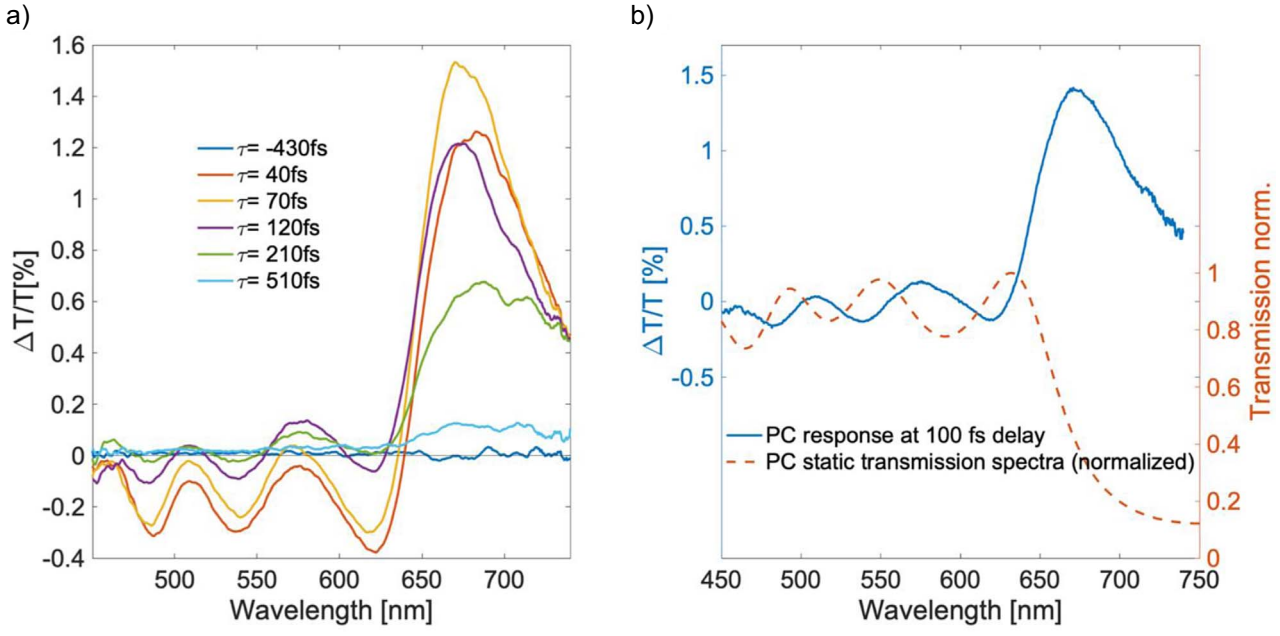

Figure 3. a) Differential transmission spectra at fixed time delay of the PC. b) Static transmission spectrum and differential transmission signal of the PC.

observe the plasmon dephasing and the creation of a non-thermalized Fermi distribution (FD). After this, within 100 fs an equilibrium hot FD is created by electron-electron scattering. The temporal resolution of our pump probe setup is about 100 fs and this does not allow us to observe the aforementioned events. However, it is possible to follow the subsequent relaxation of the hot-FD through electron-phonon scattering, that, happens in a timescale of less than 1 ps [30]. Finally, a much slower process take place which is the phonon-phonon scattering to release the heat of the lattice.

In Figure 2a the differential transmission map, as a function of wavelength and time delay, of the studied ITO film is shown. Around zero time delay we can observe the so-called Cross Phase Modulation (XPM) artifact, a coherent artifact that originates from the redistribution of the spectral component of the probe induced by the Kerr effect, a change in the refractive index caused by the strong pump pulse [31, 32]. Such fast change in the refractive index occurs only when pump and probe overlap in time on the glass substrate and is responsible for the initial positive-negative-positive signal [33]. As we discussed above the

relaxation dynamics are faster than 1 ps and can be seen in Figure 2a. For bare ITO, after the XPM we have a negative signal at every wavelength in the visible region, by exciting the plasmon and creating the hot FD we are changing the dielectric function of the material, by changing both the plasmon resonance and the refractive index [24, 34–36]. The plasmonic resonance depends on the effective mass of the carriers, ITO is a non-parabolic material, meaning that when we create a hot-FD the effective mass of the electrons changes by changing the position on the dispersion band. A second effect is the change of the ε_∞ as it was modeled by Blemker *et al.* [24], the ε_∞ change as a function of the electronic temperature of the Fermi Dirac distribution, a change of it will reflect in a change of the overall refractive index.

This leads to an ultrafast increase in the reflectivity of the ITO layer, and this is seen as a negative signal in terms of $\Delta T/T$ because more photons are reflected at the air-ITO interface. This negative signal increases toward shorter wavelengths. Around 440 nm a strong negative signal is observed, induced by the so-called inverse Moss-Burstein effect: Before excitation all the transition from the intragap state and the conduction band are neglected because the levels are already filled with electrons; when the hot-FD is created those transitions are now allowed resulting in a less transmitted probe.

In Figure 2b the differential transmission response of the ITO/TiO_2 PC is shown. We have observed a different response that has positive and negative features. As discussed above, this effect is induced by the change in the refractive index of the ITO. As for ITO film, this modulation is faster than 1 ps because it arises from the plasmon decay. By changing its refractive index the effective refractive index of the PC changes over time with a subsequent change of the PBG. This shift can create a modulation in the visible range, and an ultrafast shift is achieved.

In Figure 3a the evolution of the spectral response at various fixed delay time can be better appreciated. Remarkably, at around 510 fs the modulation has subsided. In Figure 3b the modulation of the transmission of the PC at 100 fs delay, together with its static transmission spectrum, is depicted. Here, we can better appreciate the shift of the PBG together with the shift of the side bands. By changing the thickness, refractive index and the number of layers of the PC we can change the position and shape of the resonance in the photonic bandgap. With this system we demonstrate an additional degree of freedom to modulate the optical properties of a photonic crystal: We can modulate a visible light beam, in the sub-picosecond regime, by using an infrared laser pulse. In fact, the de-excitation of the plasmon is faster than 1 ps, allowing the capability to modulate an incoming visible beam with a repetition rate faster than 1 THz.

4 Conclusion

We fabricated a PC as a multilayer of ITO and TiO_2, by designing the thickness and the number layers. An interference pattern in the visible spectra results in a modulated transmission, with the occurrence of the PBG, also called structural color [37]. The differential transmission measurements show relaxation dynamics faster than 1 ps. The change in the refractive index of ITO upon photoexcitation of the plasmon resonance can be exploited to create a PC that changes its PBG in an ultrafast time scale. This allows us to achieve all optical modulation in the visible region that can be tuned by designing the physical parameter of the PC accordingly.

Acknowledgments. This project has received funding from the *European Research Council (ERC)* under the European Union's Horizon 2020 research and innovation programme (grant agreement no. 816313). This work has been supported by Fondazione Cariplo (grant no. 2018-0979).

Supplementary Material

The supporting information of this article is available at https://jeos.edpsciences.org/10.1051/jeos/2022009/olm
Figure S1: Transmission spectra of the ITO/TiO_2 photonic crystal (experimental data in red, simulation with transfer matrix method in black). For the simulation, a Rayleigh-type scattering and a flat decrease of the transmission due to interfaces losses have been considered.
Figure S2: Transmission spectra of the ITO/TiO_2 photonic crystal (experimental data in red, simulation with transfer matrix method in black) and of a 500 nm ITO film.
Figure S3: Transmission spectrum of a 500 nm thick ITO layer up to 3000 nm.
Figure S4: Experimental setup for the ultrafast differential transmission. We have used a noncollinear optical parametric amplifier for the pump and white light generation for the probe.

References

1 John S. (1987) Strong localization of photons in certain disordered dielectric superlattices, *Phys. Rev. Lett.* **58**, 2486–2489. https://doi.org/10.1103/PhysRevLett.58.2486.
2 Yablonovitch E. (1987) Inhibited spontaneous emission in solid-state physics and electronics, *Phys. Rev. Lett.* **58**, 2059–2062. https://doi.org/10.1103/PhysRevLett.58.2059.
3 Joannopoulos J.D. (ed.) (2008) *Photonic crystals: Molding the flow of light*, 2nd edn., Princeton University Press, Princeton.
4 Sakoda K. (2005) *Optical properties of photonic crystals*, 2nd edn., Springer-Verlag, Berlin Heidelberg. https://doi.org/10.1007/b138376.
5 Komikado T., Yoshida S., Umegaki S. (2006) Surface-emitting distributed-feedback dye laser of a polymeric multilayer fabricated by spin coating, *Appl. Phys. Lett.* **89**, 061123. https://doi.org/10.1063/1.2336740.
6 Scotognella F., Monguzzi A., Cucini M., Meinardi F., Comoretto D., Tubino R. (2008) One dimensional polymeric organic photonic crystals for DFB lasers, *Int. J. Photoenergy* **2008**, 389034. https://doi.org/10.1155/2008/389034.
7 Scotognella F., Monguzzi A., Meinardi F., Tubino R. (2009) DFB laser action in a flexible fully plastic multilayer, *Phys. Chem. Chem. Phys.* **12**, 337–340. https://doi.org/10.1039/B917630F.

8 Scotognella F., Puzzo D.P., Zavelani-Rossi M., Clark J., Sebastian M., Ozin G.A., Lanzani G. (2011) Two-photon poly(phenylenevinylene) DFB laser, *Chem. Mater.* **23**, 805–809. https://doi.org/10.1021/cm102102w.

9 R. Li Voti (2018) Optimization of a perfect absorber multilayer structure by genetic algorithms, *J. Eur. Opt. Soc.-Rapid Publ.* **14**, 1–12. https://doi.org/10.1186/s41476-018-0079-7.

10 Li Y., Liu Z., Zhang H., Tang P., Wu B., Liu G. (2019) Ultra-broadband perfect absorber utilizing refractory materials in metal-insulator composite multilayer stacks, *Opt. Express* **27**, 11809–11818. https://doi.org/10.1364/OE.27.011809.

11 Choi S.Y., Mamak M., von Freymann G., Chopra N., Ozin G. A. (2006) Mesoporous Bragg stack color tunable sensors, *Nano Lett.* **6**, 2456–2461. https://doi.org/10.1021/nl061580m.

12 von Mankowski A., Szendrei-Temesi K., Koschnick C., Lotsch B.V. (2018) Improving analyte selectivity by post-assembly modification of metal-organic framework based photonic crystal sensors, *Nanoscale Horiz.* **3**, 383–390. https://doi.org/10.1039/C7NH00209B.

13 González-Pedro V., Calvo M.E., Míguez H., Maquieira Á. (2019) Nanoparticle Bragg reflectors: A smart analytical tool for biosensing, *Biosens. Bioelectron. X* **1**, 100012. https://doi.org/10.1016/j.biosx.2019.100012.

14 Megahd H., Oldani C., Radice S., Lanfranchi A., Patrini M., Lova P., Comoretto D. (2021) Aquivion–poly(N-vinylcarbazole) holistic flory-huggins photonic vapor sensors, *Adv. Opt. Mater.* **9**, 2002006. https://doi.org/10.1002/adom.202002006.

15 Megahd H., Lova P., Comoretto D. (2021) Universal Design Rules for Flory-Huggins Polymer Photonic Vapor Sensors, *Adv. Opt. Mater.* **31**, 2009626. https://doi.org/10.1002/adfm.202009626.

16 López C. (2003) Materials aspects of photonic crystals, *Adv. Mater.* **15**, 1679–1704. https://doi.org/10.1002/adma.200300386.

17 Vardeny Z.V., Nahata A., Agrawal A. (2013) Optics of photonic quasicrystals, *Nat. Photon.* **7**, 177–187. https://doi.org/10.1038/nphoton.2012.343.

18 Wiersma D.S. (2013) Disordered photonics, *Nat. Photon.* **7**, 188–196. https://doi.org/10.1038/nphoton.2013.29.

19 Chiasera A., Scotognella F., Criante L., Varas S., Valle G.D., Ramponi R., Ferrari M. (2015) Disorder in photonic structures induced by random layer thickness, *Sci Adv Mater.* **7**, 1207–1212. https://doi.org/10.1166/sam.2015.2249.

20 Feigenbaum E., Diest K., Atwater H.A. (2010) Unity-order index change in transparent conducting oxides at visible frequencies, *Nano Lett.* **10**, 2111–2116. https://doi.org/10.1021/nl1006307.

21 Heo S., Agrawal A., Milliron D.J. (2019) Wide dynamic range in tunable electrochromic Bragg stacks from doped semiconductor nanocrystals, *Adv. Funct. Mater.* **29**, 1904555. https://doi.org/10.1002/adfm.201904555.

22 Moscardi L., Paternò G.M., Chiasera A., Sorrentino R., Marangi F., Kriegel I., Lanzani G., Scotognella F. (2020) Electro-responsivity in electrolyte-free and solution processed Bragg stacks, *J. Mater. Chem. C.* **8**, 13019–13024. https://doi.org/10.1039/D0TC02437F.

23 Cerullo G., Manzoni C., Lüer L., Polli D. (2007) Time-resolved methods in biophysics. 4. Broadband pump–probe spectroscopy system with sub-20 fs temporal resolution for the study of energy transfer processes in photosynthesis, *Photochem. Photobiol. Sci.* **6**, 135–144. https://doi.org/10.1039/B606949E.

24 Blemker M.A., Gibbs S.L., Raulerson E.K., Milliron D.J., Roberts S.T. (2020) Modulation of the visible absorption and reflection profiles of ITO nanocrystal thin films by plasmon excitation, *ACS Photonics.* **7**, 1188–1196. https://doi.org/10.1021/acsphotonics.9b01825.

25 Haider A.J., Jameel Z.N., Al-Hussaini I.H.M. (2019) Review on: Titanium dioxide applications, *Energy Procedia* **157**, 17–29. https://doi.org/10.1016/j.egypro.2018.11.159.

26 Khan M.E., Khan M.M., Min B.-K., Cho M.H. (2018) Microbial fuel cell assisted band gap narrowed TiO_2 for visible light-induced photocatalytic activities and power generation, *Sci. Rep.* **8**, 1723. https://doi.org/10.1038/s41598-018-19617-2.

27 Born M., Wolf E., Bhatia A.B., Clemmow P.C., Gabor D., Stokes A.R., Taylor A.M., Wayman P.A., Wilcock W.L. (1999) *Principles of optics: Electromagnetic theory of propagation, interference and diffraction of light*, 7th edn., Cambridge University Press.

28 Scotognella F., Chiasera A., Criante L., Aluicio-Sarduy E., Varas S., Pelli S., Łukowiak A., Righini G.C., Ramponi R., Ferrari M. (2015) Metal oxide one dimensional photonic crystals made by RF sputtering and spin coating, *Ceram. Int.* **41**, 8655–8659. https://doi.org/10.1016/j.ceramint. 2015.03.077.

29 Kriegel I., Scotognella F., Manna L. (2017) Plasmonic doped semiconductor nanocrystals: Properties, fabrication, applications and perspectives, *Phys. Rep.* **674**, 1–52. https://doi.org/10.1016/j.physrep.2017.01.003.

30 Alam M.Z., De Leon I., Boyd R.W. (2016) Large optical nonlinearity of indium tin oxide in its epsilon-near-zero region, *Science* **352**, 795–797. https://doi.org/10.1126/science.aae0330.

31 Lorenc M., Ziolek M., Naskrecki R., Karolczak J., Kubicki J., Maciejewski A. (2002) Artifacts in femtosecond transient absorption spectroscopy, *Appl. Phys. B: Lasers Opt.* **74**, 19–27. https://doi.org/10.1007/s003400100750.

32 Ekvall K., van der Meulen P., Dhollande C., Berg L.-E., Pommeret S., Naskrecki R., Mialocq J.-C. (2000) Cross phase modulation artifact in liquid phase transient absorption spectroscopy, *J. Appl. Phys.* **87**, 2340–2352. https://doi.org/10.1063/1.372185.

33 Bresci A., Guizzardi M., Valensise C.M., Marangi F., Scotognella F., Cerullo G., Polli D. (2021) Removal of cross-phase modulation artifacts in ultrafast pump–probe dynamics by deep learning, *APL Photon.* **6**, 076104. https://doi.org/10.1063/5.0057404.

34 Johns R.W., Blemker M.A., Azzaro M.S., Heo S., Runnerstrom E.L., Milliron D.J., Roberts S.T. (2017) Charge carrier concentration dependence of ultrafast plasmonic relaxation in conducting metal oxide nanocrystals, *J. Mater. Chem. C.* **5**, 5757–5763. https://doi.org/10.1039/C7TC00600D.

35 Guo P., Schaller R.D., Ocola L.E., Diroll B.T., Ketterson J. B., Chang R.P.H. (2016) Large optical nonlinearity of ITO nanorods for sub-picosecond all-optical modulation of the full-visible spectrum, *Nat. Commun.* **7**, 12892_1–12892_10. https://doi.org/10.1038/ncomms12892.

36 Paternò G.M., Iseppon C., D'Altri A., Fasanotti C., Merati G., Randi M., Desii A., Pogna E.A.A., Viola D., Cerullo G., Scotognella F., Kriegel I. (2018) Solution processable and optically switchable 1D photonic structures, *Sci Rep.* **8**, 1–8. https://doi.org/10.1038/s41598-018-21824-w.

37 Kinoshita S., Yoshioka S., Miyazaki J. (2008) Physics of structural colors, *Rep. Prog. Phys.* **71**, 076401. https://doi.org/10.1088/0034-4885/71/7/076401.